Electronic Supplementary Material (ESI) for Journal of Materials Chemistry C.

Supplementary Information

Unexpectedly flexible graphene nanoribbons with a polyacene ladder skeleton

Marvin T. Unruh,[a] Ullrich Scherf,[a] Hilke Bahmann,[b] Ana Clara B. Rodrigues,[c] Carla Cunha,[c] J. Sérgio Seixas de Melo,[c] Jakob Schedlbauer[d] and John M. Lupton[d]

[a] Bergische Universität Wuppertal, Macromolecular Chemistry group (*buwMakro*) and Wuppertal Center for Smart Materials and Systems (*CM@S*), Gauss-Str. 20, D-42119 Wuppertal, Germany, Email: scherf@uni-wuppertal.de

[b] Universität des Saarlandes, Physical and Theoretical Chemistry, Campus Saarbrücken B 2.2, D-66123 Saarbrücken, Germany, Email: hilke.bahmann@uni-saarland.de

[c] University of Coimbra, CQC, Department of Chemistry, Rua Larga, 3004-535, Coimbra, Portugal. Email: sseixas@ci.uc.pt

[d] Institut für Experimentelle und Angewandte Physik, Universität Regensburg, D-93053 Regensburg, Germany. Email: john.lupton@ur.de

Table of contents

General Methods

All reactions were carried out in argon atmosphere. The solvents used were of commercial quality (HPLC grade). If necessary, the solvents were dried using common procedures. Unless otherwise indicated, all reagents were obtained from commercial suppliers and were used without further purification. All reactions were carried out under an argon atmosphere by use of standard Schlenk techniques. ^{1}H and ^{13}C NMR spectra were recorded on Bruker Avance 400 or Avance III 600 spectrometers. Gel permeation chromatographic analysis (GPC) utilized PS-columns (two columns, 5 µm gel, pore widths mixed bed linear) connected with UV/Vis and RI detection. All GPC analyses were performed on solutions of the polymers in chloroform at 30 °C (concentration of the polymer: approx. 1.0 g L^{-1}). The calibration was based on polystyrene standards with narrow molecular weight distribution.

Polymer Synthesis

A) Suzuki coupling towards precursor polymer ***P1***

In a microwave vessel the dibromo monomer (2,5-dibromo-4',4''-bis-*n*-decyl-terephthalophenone **M2** : 1 eq, 333 mg, 0.459 mmol), the diborylated monomer (3,7-di-tert-butyl-9,10-dihydroanthracene-1,5-bispinacolatoborate **M1**: 1 eq, 250 mg, 0.459 mmol), potassium carbonate (5 eq, 317 mg, 2.3 mmol) Aliquat 336 (0.05 Eq.) and tetrakis(triphenylphosphine)palladium(0) (0.05 eq, 26.5 mg, 0.023 mmol) were filled in under argon atmosphere. The solids were dissolved in a mixture of toluene (6 mL) and degassed water (3 mL) and stirred at 80 °C for 72 h. Afterwards the solution was cooled down, diluted with chloroform and water, and washed with aqueous 2M HCl-solution. The solvents were removed under reduced pressure and the crude polymer was dissolved in a small amount of chloroform. Next, the polymer was precipitated into cold methanol and purified by Soxhlet extraction (methanol, acetone, chloroform). The chloroform fraction was used for the next step.

^{1}H NMR spectrum (600 MHz, $C_2D_2Cl_4$, 353 K) δ = 7.63 – 7.40 (m, 6H), 7.15 – 6.82 (m, 8H), 3.78 (s, 4H), 2.44 (s, 4H), 1.61 – 1.38 (m, 4H), 1.32 – 1.17 (m, 28H), 1.18 – 1.06 (m, 18H), 0.85 (t, *J* = 6.6 Hz, 9H).

^{13}C NMR spectrum (151 MHz, $C_2D_2Cl_4$, 353 K) δ = 200.20, 151.33, 144.59, 142.33, 140.25, 139.81, 138.57, 135.22, 133.41, 132.82, 131.27, 128.52, 127.25, 123.59, 39.04, 37.82, 37.33, 35.00, 34.64, 34.42, 33.86, 32.70, 32.65, 32.50, 32.38, 25.75, 17.14.

P1 Fraction	M_n [g/mol]	M_w [g/mol]	M_n/M_w	Yield [mg]	Yield [%]	Degree of Polymerization P_n
Chloroform	12000	17400	1.45	193	48	14

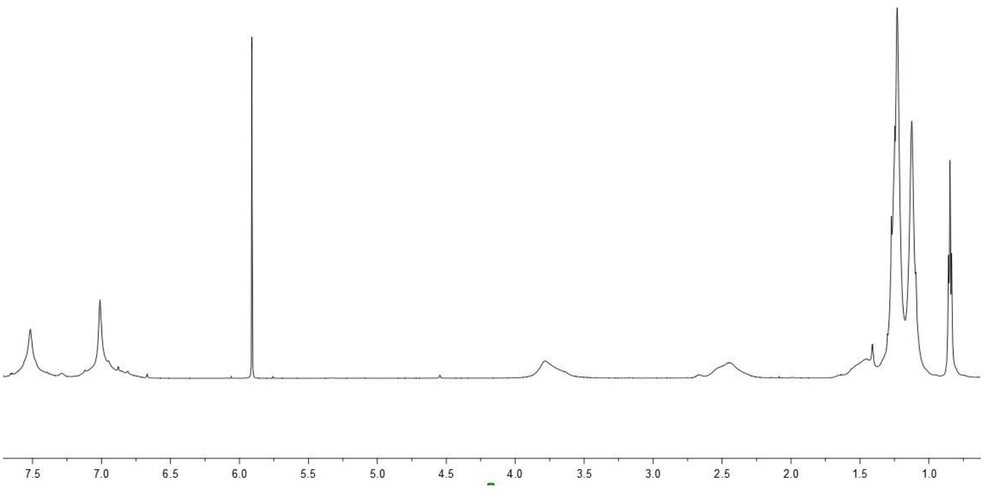

Figure S1a. ^{1}H-NMR spectrum of the single-stranded precursor polymer **P1** (solvent: $C_2D_2Cl_4$).

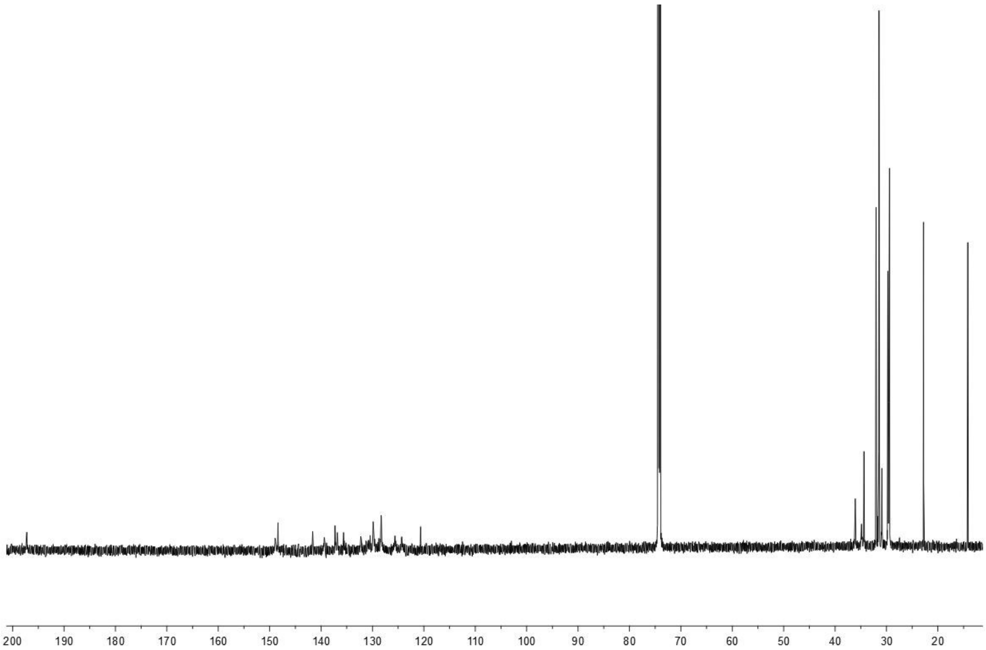

Figure S1b. ^{13}C-NMR spectrum of the single-stranded precursor polymer **P1** (solvent: $C_2D_2Cl_4$).

*B) Post-Polymerization Cyclization into **PAL** (**P2**)*

A solution of the single-stranded precursor polymer **P1** (100 mg) and KOt-Bu (100 mg) in DMF (20 mL) was flushed with argon and stirred at 80 °C for 24 h. Then, water was added, and the mixture was extracted with chloroform. The solvents were removed under reduced pressure and the ladder polymer was dissolved in a small amount of chloroform. Finally, the polymer was precipitated into cold methanol and dried.

^{1}H NMR spectrum (600 MHz, $C_2D_2Cl_4$, 353 K) δ = 8.93 (s), 8.22 (s), 8.04 (s), 7.64 – 7.42 (m), 2.78 (s), 1.81 (s), 1.59 – 1.34 (m), 1.34 – 1.20 (m), 1.17 – 1.02 (m), 0.98 – 0.83 (m).

Recording of a suitable ^{13}C NMR spectrum of **PAL** (**P2**) with an acceptable signal-to-noise ratio was not possible due to solubility limitations.

M_n [g/mol]	M_w [g/mol]	M_n/M_w	Yield [mg]	Yield [%]	Degree of Polymerization P_n
11900	20000	1.68	63	64	15

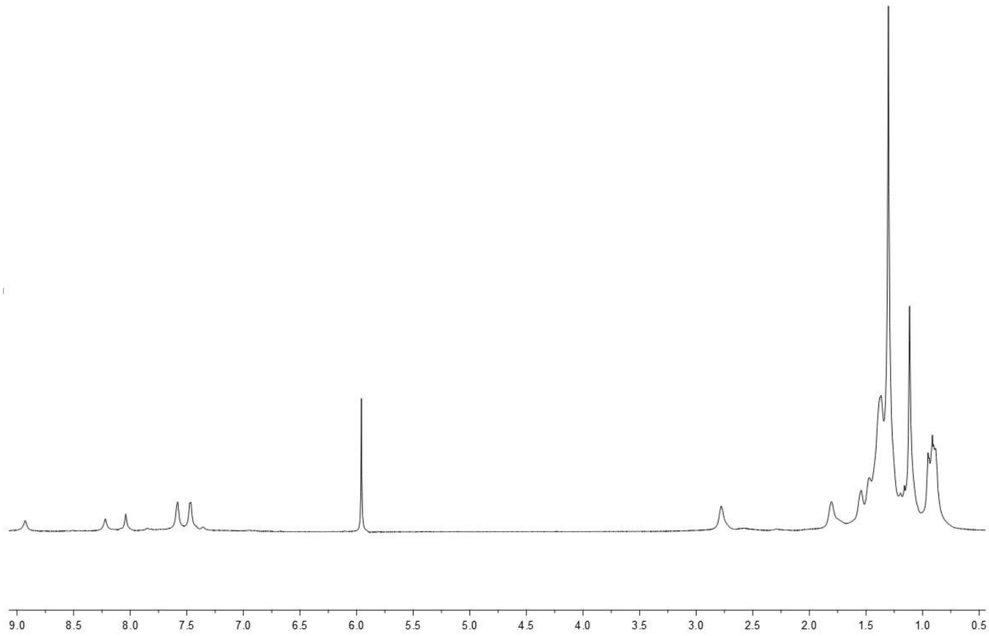

Figure S2. ^{1}H-NMR spectrum of the ladder polymer **PAL** (**P2**; solvent: $C_2D_2Cl_4$).

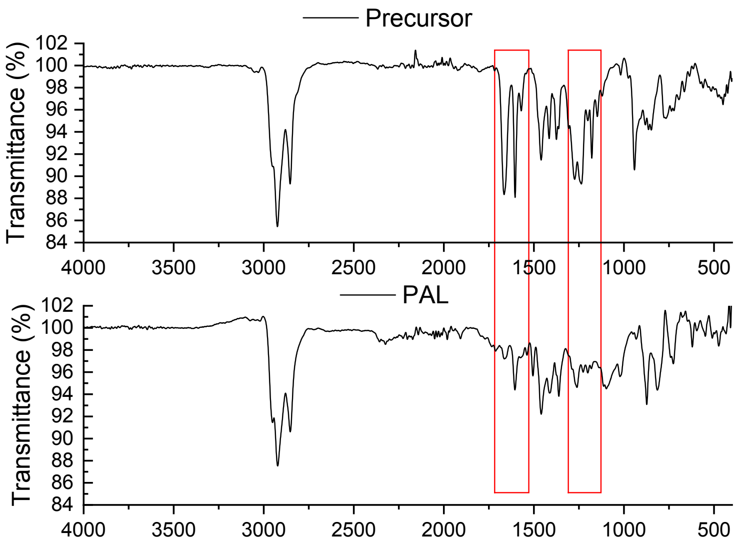

Figure S3. IR spectra of the single-stranded precursor polymer **P1** and the final ladder polymer **PAL** (**P2**): Please notice the nearly complete disappearance of the carbonyl-related vibrations (red boxes). A very small portion of remaining CO signals may be connected to the occurrence of carbonyl end-groups.

Spectroscopy

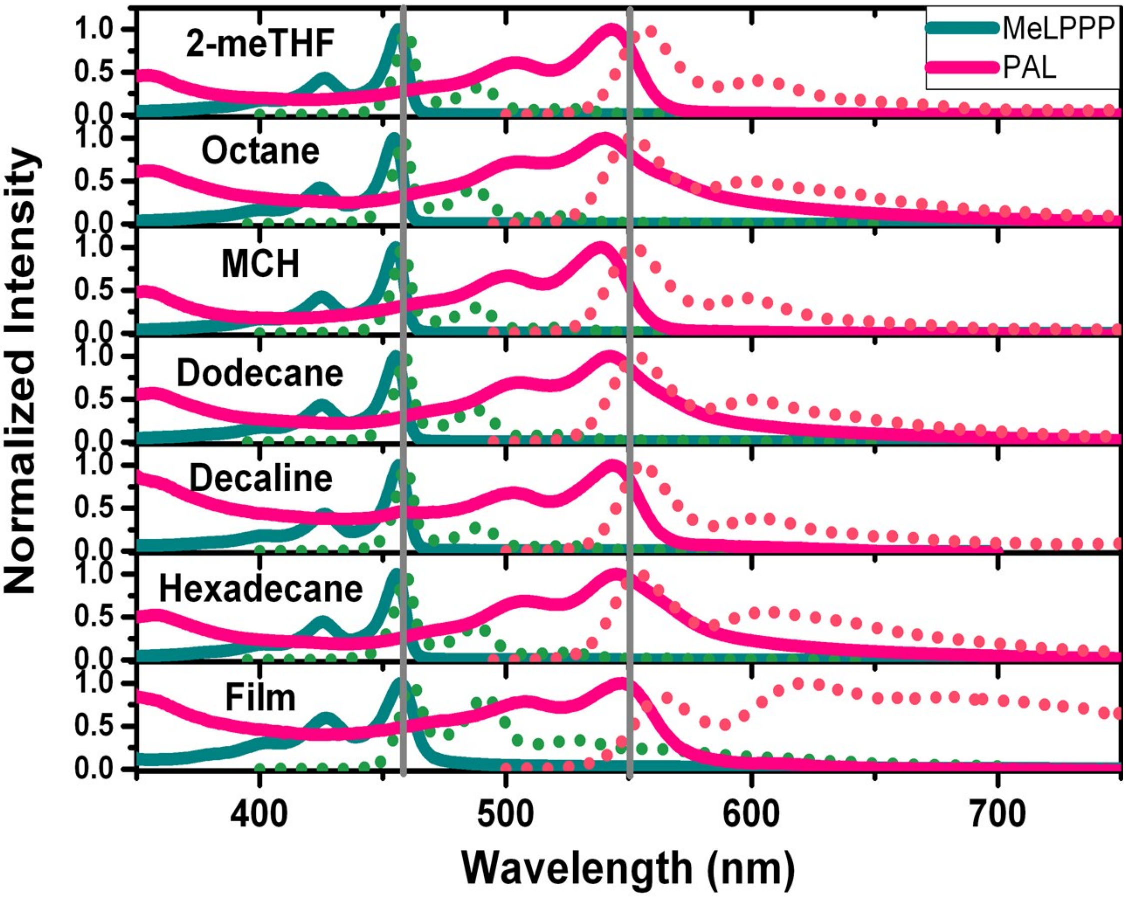

Figure S4. Comparison of the normalize room temperature absorption (plain line) and photoluminescence (dashed line) spectra of **MeLPPP** and **PAL** (**P2**) in solvents and in spin-coated films. The vertical grey lines are visual guides to show small displacements of the 0-0 bands.

Table S1. Time resolved photoluminescence data (lifetimes, τ_i, pre-exponential factors, a_i, and chi-squared values, χ^2) for **MeLPPP** obtained with ps-TCSPC technique collected at several wavelengths; λ_{exc} = 395 nm at T = 293 K.

Medium	λ_{em} (nm)	τ_1 (ns)	τ_2 (ns)	τ_3 (ns)	a_1 (%C_1)	a_2 (%C_2)	a_3 (%C_3)	χ^2
2-meTHF	480	0.34	-	-	1.00	-	-	1.01
	520							1.03
MCH	480	0.34	-	-	1.00	-	-	0.85
	520							0.83
Decaline	480	0.38	-	-	1.00	-	-	0.83
	520							1.00
Film	480	0.52	0.167	0.960	0.784 (50)	0.211 (44)	0.005 (6)	1.00

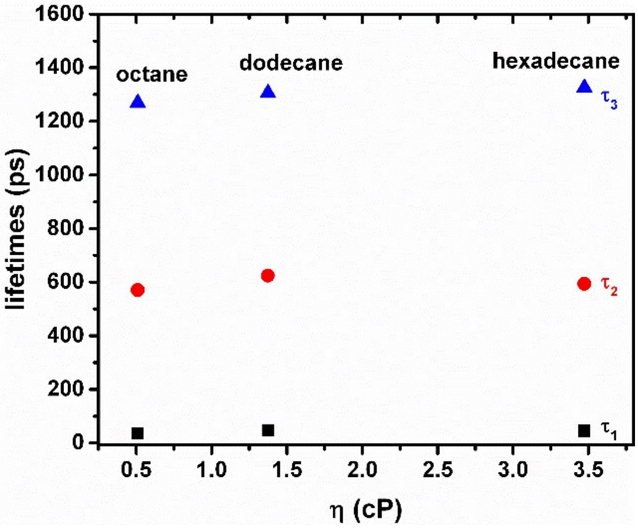

Figure S5. Viscosity dependence of the fluorescence decay times (τ_i) for **PAL** (**P2**) obtained with λ_{exc} = 395 nm at room temperature.

Table S2. Photophysical data for **PAL** (**P2**); photoluminescence quantum yield, ϕ_F, PL lifetime, τ_F, and rate constants, k_F and k_{NR}) in different solvents.

Medium	**ϕ_F**	**τ_F[a] (ns)**	**k_F[b] (ns^{-1})**	**k_{NR}[b] (ns^{-1})**
2-meTHF	0.53	0.849	0.624	0.554
Octane	0.32	0.570	0.561	1.193
MCH	0.53	0.862	0.615	0.545
Dodecane	0.27	0.624	0.433	1.170
Decaline	0.54	0.889	0.619	0.506
Hexadecane	0.27	0.594	0.455	1.230
Film	0.076	0.980	0.078	0.943

[a] Major decay component obtained in different solvents.

[b] $k_F = \frac{\phi_F}{\tau_F}$; $k_{NR} = \frac{1-\phi_F}{\tau_F}$;

Table S3. Room temperature spectroscopic/photophysical data for **MeLPPP** (absorption λ^{abs} and photoluminescence emission λ^{em} maxima, Stokes-shifts, Δ_{SS}, PL quantum yields, ϕ_F, Pl lifetimes, τ_F, and rate constants, k_F and k_{NR}) in different solvents.

Solvent	**λ^{abs} (nm)**	**λ^{em} (nm)**	**ΔSS (cm^{-1})**	**ϕ_F**	**$k_R \times 10^{-9}$ (s^{-1})**	**$k_{NR} \times 10^{-7}$ (s^{-1})**
2-meTHF	400/426/456	460/489/524	191	0.922	2.25	19.0
MCH	401/425/455	458/487/524	144	0.853	2.44	42.0
Decaline	401/427/457	459/488/525	95	0.962	3.01	11.9

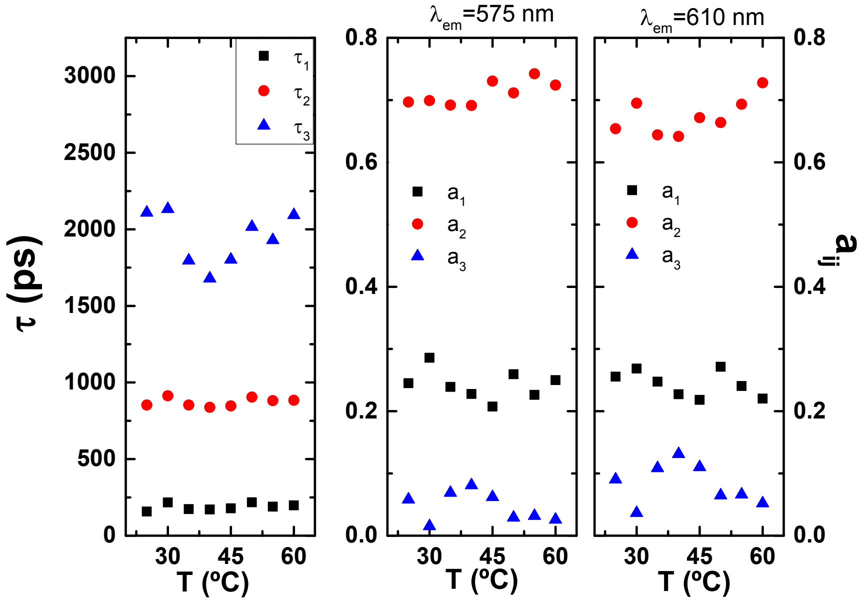

Figure S6. Temperature dependence of the PL decay times (τ_i) and pre-exponential factors (a_{ij}) for **PAL** (**P2**) in decaline solution, obtained with λ_{exc}=395 nm and λ_{em}= 575 and 610 nm.

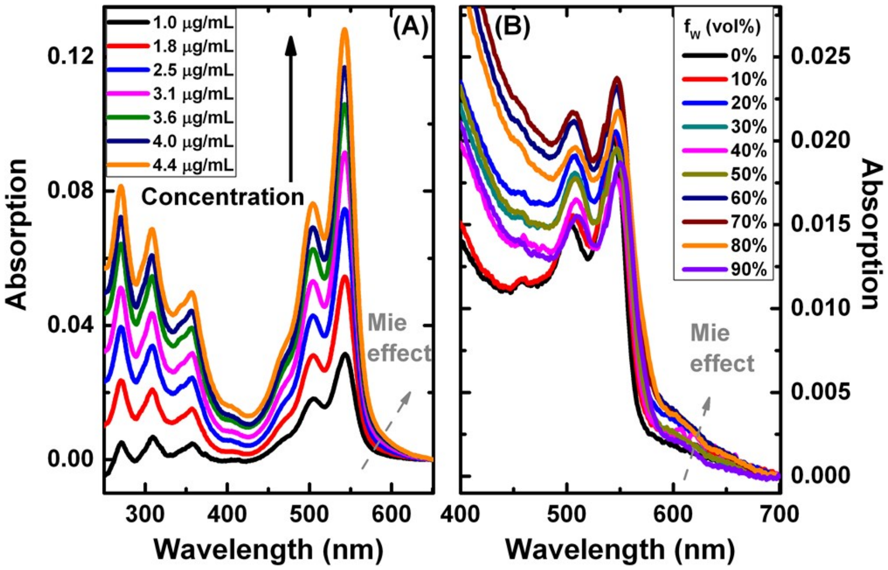

Figure S7. Dependence of the absorption spectra of **PAL** (**P2**) on the concentration (left hand panel, solvent: MCH) and on the water content in THF/water mixtures (right hand panel).

Table S3. Time resolved PL data for **PAL** (**P2**; PL lifetimes, τ_i, pre-exponential factors, a_{ij}, and chi-squared values, χ^2) obtained with ps-TCSPC technique in THF/water mixtures; λ_{exc} = 395 nm at T = 293 K.

Solvent	λ_{em}	τ_1	τ_2	τ_3	a_1	a_2	a_3	χ^2	C_1 (%)	C_2(%)	C_3(%)
100% THF	575	0.118	0.827	2.05	0.413	0.560	0.027	1.01	9	82	10
	610				0.664	0.753	0.081	1.08	9	72	19
	630				0.394	0.472	0.134	1.06	7	55	39
90%THF:10%W	575	0.086	0.881	2.35	0.484	0.495	0.020	0.93	8	83	9
	610				0.461	0.505	0.034	1.04	7	79	14
	630				0.351	0.582	0.067	1.14	4	73	23
70%THF:30%W	575	0.026	0.307	1.08	0.966	0.022	0.012	1.12	57	15	28
	610				0.740	0.160	0.100	1.00	11	28	61
	630				0.460	0.269	0.271	0.99	3	21	76
50%THF:50%W	575	0.058	0.495	1.50	0.931	0.058	0.011	0.71	54	29	17
	610				0.741	0.151	0.108	0.96	15	27	58
	630				0.512	0.205	0.283	1.08	5	18	76
30%THF:70%W	575	0.028	0.398	1.24	0.928	0.069	0.003	1.06	46	48	6
	610				0.774	0.150	0.075	1.09	13	34	53
	630				0.509	0.247	0.244	1.07	3	24	73
20%THF:80%W	575	0.066	0.452	1.72	0.783	0.201	0.016	0.68	30	53	16
	610				0.611	0.278	0.111	0.89	11	35	54
	630				0.433	0.255	0.312	1.08	4	17	79

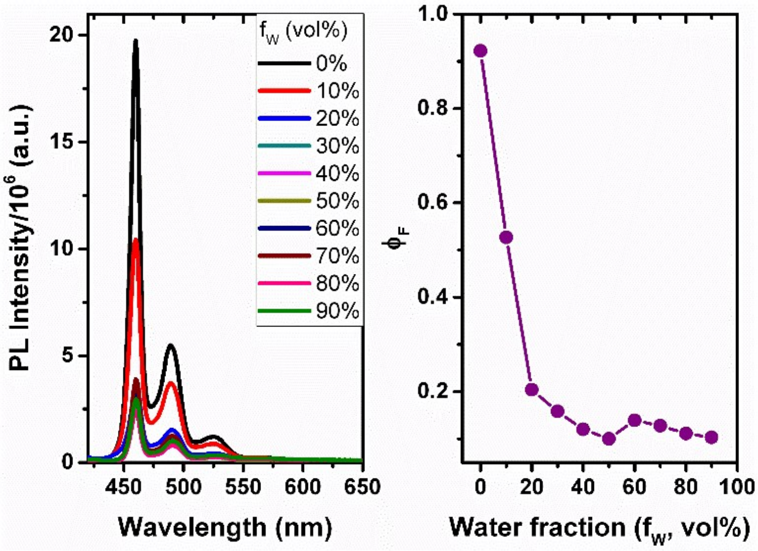

Figure S8. Steady state PL spectra of **MeLPPP** in THF/water mixtures with increasing water content (left)and PL quantum yields in THF/water mixtures with increasing water content (right) at T = 293 K.

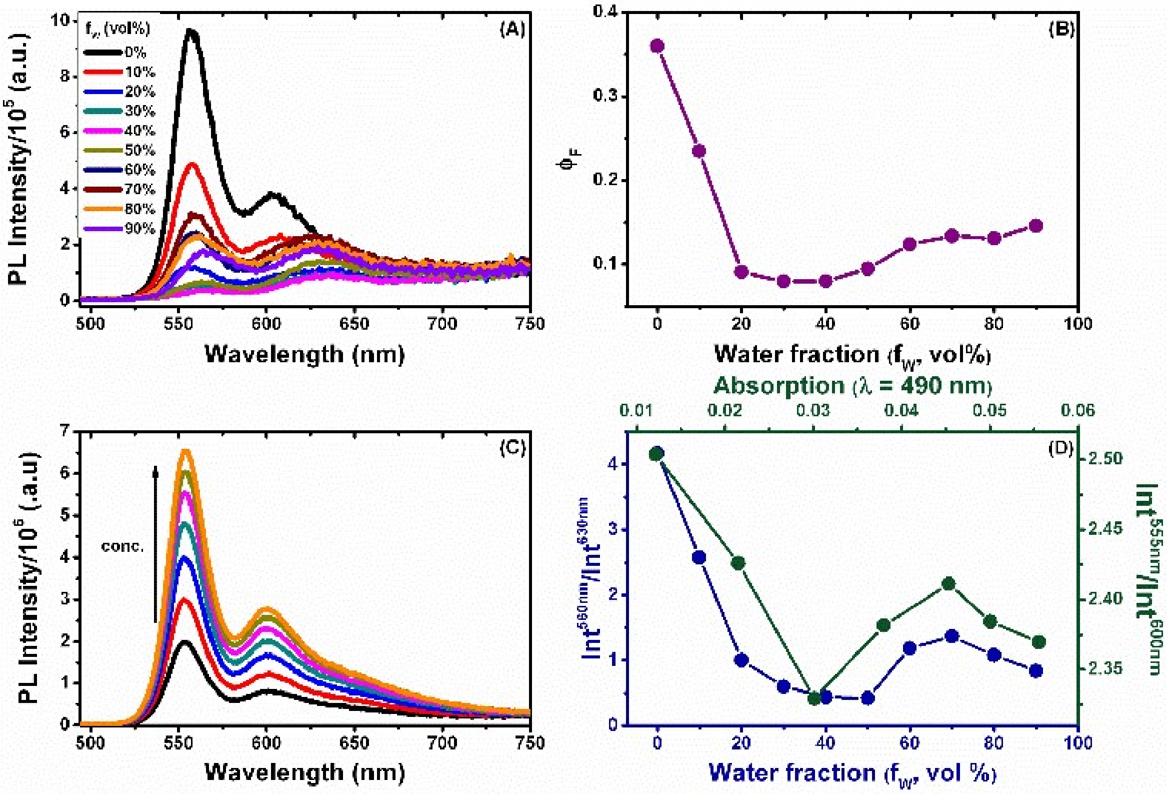

Figure S9. Steady state PL spectra of **PAL** (**P2**) in THF/water mixtures with increasing water content (A) and in pure THF for increasing concentration (C), PL quantum yields of **PAL** (**P2**) in THF/water mixtures with increasing water content (B), and ratio of the vibronic emission peaks (580/630 nm, and 555/600 nm bands) in THF/water mixtures for **PAL** (**P2**) at T = 293 K (D).

Table S4. PL data for **PAL** (**P2**; PL lifetimes, τ_i, pre-exponential factors, a_{ij}, and chi-squared values, χ^2) obtained with ps-TCSPC technique at different temperature; λ_{exc} = 395 nm.

T (^{o}C)	λ_{em}	τ_1	τ_2	τ_3	a_1	a_2	a_3	χ^2	C_1 (%)	C_2(%)	C_3(%)
25	575	158	853	2109	0.245	0.697	0.058	1.09	5	79	16
	610				0.256	0.654	0.090	1.11	5	71	24
30	575	227	947	2965	0.286	0.699	0.015	1.15	8	86	6
	610				0.269	0.695	0.036	1.05	7	80	13
35	575	173	853	1796	0.239	0.692	0.069	1.05	5	78	16
	610				0.248	0.644	0.108	0.91	5	70	25
40	575	171	838	1679	0.228	0.691	0.081	1.03	5	77	18
	610				0.227	0.642	0.131	0.99	5	67	28
45	575	178	847	1802	0.208	0.730	0.062	0.95	5	81	15
	610				0.218	0.672	0.110	1.05	5	71	25
50	575	218	905	2016	0.259	0.711	0.029	0.92	7	85	8
	610				0.271	0.664	0.065	1.05	7	76	17
55	575	189	881	1930	0.226	0.742	0.032	0.96	6	86	8
	610				0.240	0.693	0.066	1.06	6	78	16
60	575	198	884	2093	0.250	0.724	0.026	1.01	7	86	7
	610				0.220	0.728	0.052	1.03	5	81	14
65	575	205	859	1687	0.214	0.733	0.053	0.92	6	83	12
	610				0.238	0.665	0.097	1.01	6	73	21

Computational details and quantum chemical calculations

All density functional theory calculations were performed with the TURBOMOLE program package[1] using the def2-SVP basis set,[2] the *ri*-approximation and *m3* grids. The ground state structures were optimized with the B3LYP functional[3] and for the excitation energies the CAM-B3LYP functional[4] was employed along with the standard settings for linear-response time-dependent DFT in TURBOMOLE. For the monomer and the dimer, the harmonic force constants were determined to distinguish between ground and transition states.

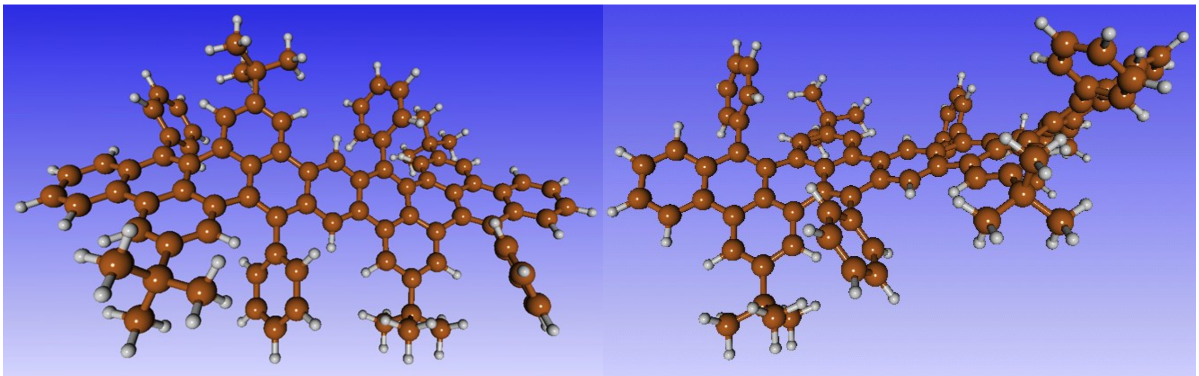

Figure S10: Optimized ground state structures of the dimer model for polymer **PAL** (**P2**).

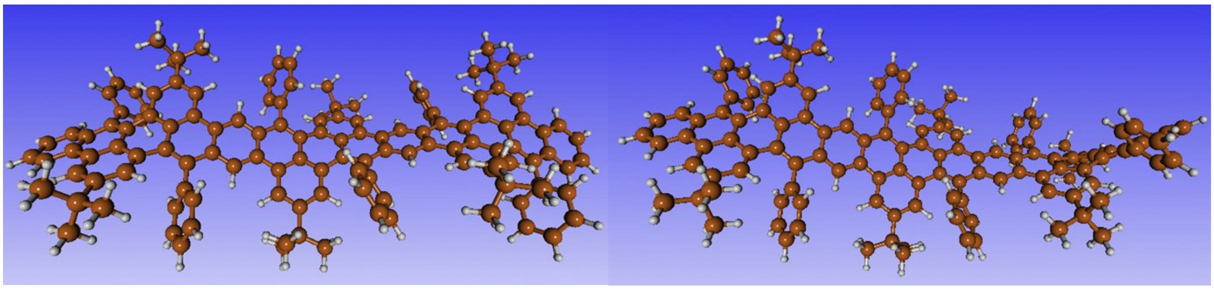

Figure S11: Optimized structures of the trimer model for for polymer **PAL** (**P2**).

---

[1] TURBOMOLE V7.5 2019, a development of the University of Karlsruhe and Forschungszentrum Karlsruhe GmbH, 1989-2007, TURBOMOLE GmbH, since 2007; available from http://www.turbomole.com

[2] F. Weigend and R. Ahlrichs, *Phys. Chem. Chem. Phys.* 2005, **7**, 3297

[3] A. D. Becke, J. Chem. Phys. 1993, **98**, 5648; C. Lee, W. Yang, R. G. Parr, *Phys. Rev. B* 1988, **37**, 785

[4] T. Yanai, D. Tew, N. Handy, *Chem. Phys. Lett.* 2004, **393**, 51

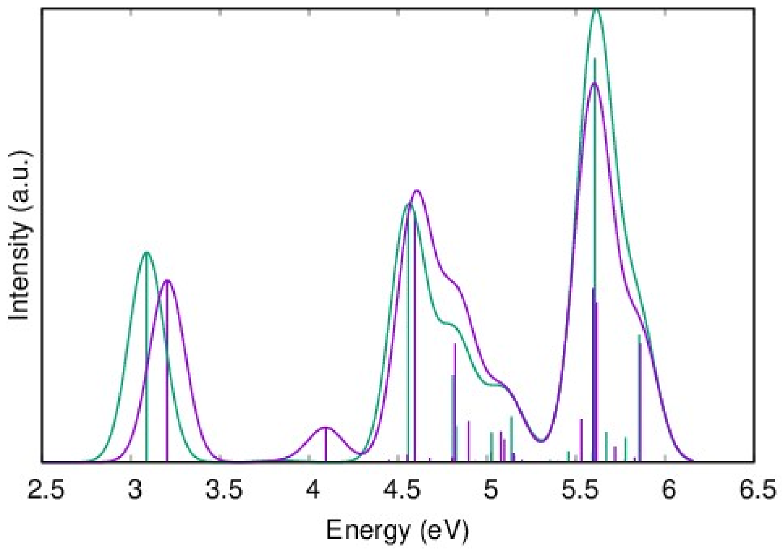

Figure S12: Calculated absorption spectra of the monomer model for polymer **PAL** (**P2**). Green line: *aa*-configuration (transition state), purple line: *ab*-configuration